

A SLOT ANTENNA-COUPLED MICROBOLOMETER FOR DETECTION AT 94 GHz

M. Abdel-Rahman^{1,*}, N. Al-Khalli², A. Kusuma³, and N. Debbar²

¹Prince Sultan Advanced Technologies Research Institute (PSATRI), College of Engineering, King Saud University, P. O. Box 800, Riyadh 11421, Saudi Arabia

²Electrical Engineering Department, College of Engineering, King Saud University, P. O. Box 800, Riyadh 11421, Saudi Arabia

³P.T. Telekomunikasi Indonesia Tbk, Jl. Gatot Subroto Kav. 52, Jakarta Selatan, Indonesia

Abstract—In this paper, we report on the design, fabrication and characterization of a slot antenna on a quarter wavelength silicon (Si) substrate coupled to an uncooled titanium (Ti) microbolometer for detection at 94 GHz. The detector was fabricated using conventional photolithographic and microfabrication techniques. The detector exhibited a voltage responsivity (R_v) of 0.779 V/W, a noise equivalent power (NEP) of 10.2 nW/ $\sqrt{\text{Hz}}$, and a time constant (τ) of 3.88 μsec .

1. INTRODUCTION

Antenna-coupled microbolometers are widely investigated as millimeter wave (MMW) detectors [1–5] due to their low cost and ease of fabrication as compared to detectors based on monolithic microwave integrated circuit (MMIC) technologies [6]. An antenna-coupled microbolometer operates such as a resonant antenna serves to collect the incident MMW radiation; the antenna resonant currents are then dissipated in a microbolometer located at the feed of the antenna causing joule heating in the microbolometer element. This joule heating translates into a resistance change of the microbolometer. The resistance change is sensed by biasing the microbolometer element with a constant current and monitoring the voltage change resulting from the incident

Received 25 April 2012, Accepted 4 June 2012, Scheduled 11 June 2012

* Corresponding author: Mohamed Abdel-Rahman (mabdelrahman@ksu.edu.sa).

radiation. The antenna-coupled microbolometer voltage responsivity (R_v) is defined as the ratio between the induced electric voltage and the incident MMW power. It can be expressed as [7]:

$$R_v = \frac{I_{\text{bias}} R \alpha \eta \beta}{G \sqrt{1 + \omega^2 \tau^2}}, \quad (1)$$

where I_{bias} is the microbolometer bias current, R the microbolometer resistance, α the temperature coefficient of resistance (TCR) of the microbolometer material, G the thermal conductance of the microbolometer, η the optical absorption coefficient, β the fill factor, ω the modulation frequency, and τ the time constant of the microbolometer. The term η , in the case of antenna-coupled microbolometer, accounts for the antenna reception efficiency and the coupling efficiency between the antenna and the microbolometer. Noise equivalent power (NEP), another figure of merit of the antenna coupled microbolometer, is defined as the amount of radiant power collected on a detector that will produce a signal to noise ratio of 1. NEP is given by [8]:

$$NEP = \frac{V_n}{R_v}, \quad (2)$$

where V_n is the noise voltage of the antenna-coupled microbolometer, and R_v is its voltage responsivity as defined in Equation (1).

In this paper, we report on the design, fabrication, and characterization of a single element slot antenna on a quarter wavelength silicon (Si) substrate coupled to an uncooled titanium (Ti) microbolometer.

2. DETECTOR DESIGN AND FABRICATION

The antenna was designed for an operating frequency of 94 GHz. The antenna ground plane length and width are $3.13\lambda_o$ (λ_o is the free space wavelength). The ground plane size is chosen so as to act as a single element detector in an $f/1.3$ MMW imaging system that will be designed in the future. The designed antenna is a slot antenna on a quarter wavelength ($231 \mu\text{m}$) high resistivity ($\rho > 5000 \Omega\cdot\text{cm}$) Si substrate; this choice of substrate thickness is known to provide the highest possible gain [9]. The Si substrate is coated with a $1.2 \mu\text{m}$ layer of silicon dioxide (SiO_2) for the purpose of electrical and thermal isolation. The antenna has a length of $0.74\lambda_d$ (λ_d is the dielectric wavelength, $\lambda_d = \lambda_o/\sqrt{\epsilon_r}$) and a length to width ratio of 6.27. Two DC cuts, $10 \mu\text{m}$ in width, were made to allow for microbolometer bias and signal readout. Antenna simulations were made using an FDTD-based software package, SEMCAD-X.

Although Niobium (Nb) is the most widely used microbolometer material for MMW antenna-coupled microbolometers; Ti was chosen as the microbolometer material in this work. Both Nb and Ti possess the proper electrical resistivity for producing impedance matched microbolometers within the detectors' geometrical constraints, and they both possess similar TCR values. Nevertheless, Ti has approximately 2.5 times less thermal conductivity (the comparison was made for bulk films) than Nb suggesting the potential to realize higher responsivity using Ti. The microbolometer was designed with dimensions of $10\ \mu\text{m} \times 3\ \mu\text{m} \times 70\ \text{nm}$ and it was placed at the center of the slot antenna.

The antenna ground plane was formed by depositing a 100 nm layer of aluminum (Al). Aluminum was deposited using DC magnetron sputtering at 150 W of power at a chamber base pressure of 7×10^{-7} Torr and an argon (Ar) pressure of 3 m Torr. Rohm & Haas S1813 photoresist was then spun at 4500 rpm for 30 sec. The resist was exposed for 3 sec. at 175 W of ultraviolet power at a wavelength of 365 nm using an NXQ 4004 contact mask aligner. The resist was then developed for 90 sec. in Rohm & Haas MIF 319 developer. With the patterned resist acting as a mask, Ar ions were used for sputter etching the Al ground plane in the resist free areas and thus forming the slot antenna structures and the dc bias cuts. Sputter etching was performed at an RF power of 30 W, a substrate holder rotation of 40 rpm, a chamber base pressure of 7.5×10^{-7} Torr and an Ar pressure of 3 m Torr. Sputter etching was performed for 30 min. on two steps with a cool down interval of 15 min. in order to prevent the resist from thermal cross linking. The remaining resist was then removed using Rohm & Haas 1165 remover with the aid of ultrasonic power at 80°C for 8 minutes. A second mask was used for microbolometer patterning. Rohm & Haas S1813 photoresist was spun, exposed in accordance with the above process. The exposed resist was soaked in Toluene for 5 min. prior to development. Resist was then developed for 80 sec. Further, a 70 nm thin film of Ti was deposited using DC magnetron sputtering at 150 W of DC power at a chamber base pressure of 5×10^{-7} Torr and an Ar pressure of 3 m Torr. Titanium metal was then lifted off by overnight soaking in Rohm & Haas 1165 remover. An optical microscope photograph for the fabricated detector is shown in Fig. 1.

3. TESTING AND CHARACTERIZATION

A network analyzer transmitter/receiver module was utilized as the source of millimeter wave radiation. A 25 dB gain W-band horn antenna was connected to the network analyzer port and it was used to irradiate the detector. A PIN switch or an optical chopper was used to

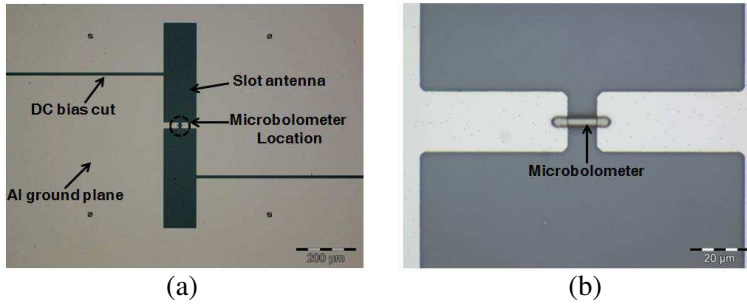


Figure 1. An optical microscope photograph of the fabricated device, (a) the slot antenna and (b) the microbolometer.

modulate the radiation falling onto the detector. Voltage responsivity (R_v) and noise equivalent power (NEP) measurements were made using the PIN switch at a modulation frequency of 1 kHz. Time constant measurements were also performed using the PIN switch. For radiation pattern measurements, a 2-blade optical chopper was used for modulating the MMW beam at 100 Hz. All the measurements were taken at the point where the polarization of the incident wave produced the highest voltage response. The power density of the radiation incident on the detector is 9.5 W/cm^2 . The detector was mounted on 3-axis (x , y , and z) micropositioning stages for precise positioning at the center of the irradiating beam. The detector was biased at 1.38 mA. The modulated detector response signal was then preamplified using a low noise preamplifier at a voltage gain of 1 and further amplified at a voltage gain of 952. The high amplification was used in order to raise the signal level above the signal analyzer noise level. All bias and amplification circuitry were battery operated to avoid power supply noise. The test setup is shown in Fig. 2. The amplified modulated detector response signals were then captured using a signal analyzer. Fig. 3 shows the detected signal spectrum.

The voltage responsivity (R_v) of the detector was found to be 0.779 V/W and the signal to noise ratio (SNR) was measured to be 70. All of which resulted in a noise equivalent power (NEP) of $10.2 \text{ nW}/\sqrt{\text{Hz}}$.

For reception pattern measurements, the detector was mounted on a manual rotational stage in the setup implemented and shown in Fig. 2, and was subject to angular variations of 2° . The signal was recorded at each angular variation. The normalized detected signal in both E - and H -planes along with the normalized simulated gain are shown in Fig. 4. The ripply behavior of the measured radiation pattern is believed to be due to the reflections caused by the high edges of the ceramic chip carrier structure surrounding the detector. The

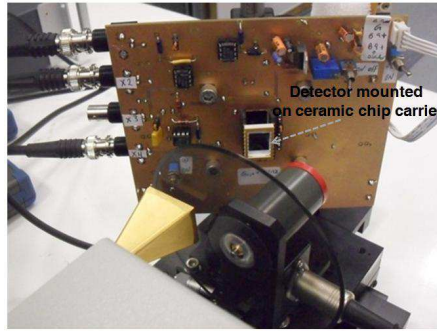


Figure 2. Experimental setup for antenna-coupled microbolometer characterization; the detector is being obliquely irradiated by a horn antenna beam that is modulated by an optical chopper, during radiation pattern measurement.

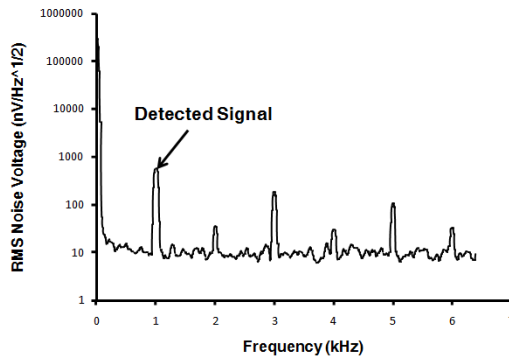


Figure 3. Measured RMS noise voltage spectrum.

ceramic material of the chip carrier was intentionally removed below the detector to avoid it being acting as a substrate. However, the mounting points and the surrounding chip carrier structure will still affect the radiation pattern and probably the resonance of the antenna structure. It can be deduced that the carrier should be included in the simulation.

Time constant measurements were performed by varying the modulation frequency of the PIN switch using a function generator and measuring the response of the detector using a lock-in amplifier that is referenced at the PIN switch’s modulation frequency. Accordingly, normalized detector response versus modulation frequency was measured. The normalized detector response as a function of the modulation frequency is shown in Fig. 5. The 3-dB frequency ($f_{0.7}$)

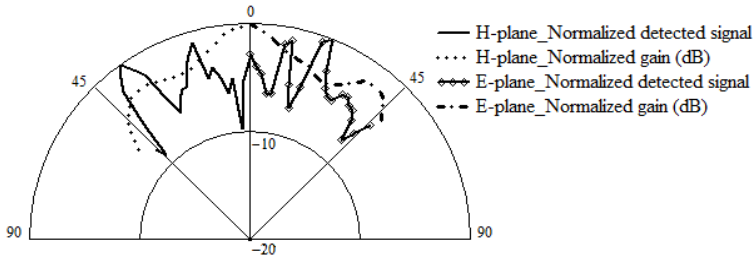


Figure 4. Measured *E*- and *H*-plane reception patterns for a MMW slot antenna-coupled Ti microbolometer. Simulated normalized antenna gain is plotted for comparison.

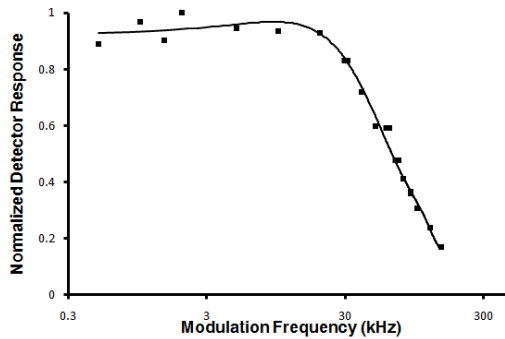


Figure 5. Normalized detector response versus modulation frequency for slot antenna-coupled Ti microbolometer on Si/SiO₂ substrate.

was read from the measured response. This value of the frequency can be used to calculate the time constant (τ) of the microbolometer according to the well known relation $\tau = 1/(2 \cdot \pi \cdot f_{0.7})$. For our detector, the time constant (τ) was calculated to be 3.88 μsec . This time constant is suitable for employing the detector for video frame rate imaging.

4. SUMMARY

In this paper, we have designed, fabricated and characterized a single element slot antenna on a quarter wavelength Si substrate coupled to an uncooled Ti microbolometer for detection at 94 GHz. The detector was fabricated using conventional photolithography, dry etching and metal liftoff techniques. The detector measured a voltage responsivity (R_v) of 0.779 V/W, a noise equivalent power (NEP) of 10.2 nW/ $\sqrt{\text{Hz}}$, and a time constant (τ) of 3.88 μsec . Better performance can be achieved by thermally isolating the microbolometer on an air bridge but this means a more complicated fabrication process and a slower

time response. To maintain simplicity of fabrication and fast response time, peltier cooling could be another simple low cost approach that may contribute further to improving the detector performance.

ACKNOWLEDGMENT

This work was supported by the Annual Grants Program at KACST under grant No. AT 4-13 and by the National Science, Technology and Innovation Plan (NSTIP) at King Saud University, Saudi Arabia under grant No. 09-ELE666-02.

REFERENCES

1. Nolen, S., J. A. Koch, N. G. Paulter, C. D. Reintsema, and E. N. Grossman, "Antenna-coupled niobium bolometers for mm-wave imaging arrays," *SPIE Proceedings Conference on Terahertz and Gigahertz Photonics*, 279–286, July 1999.
2. Heston, J. G., J. M. Lewis, S. M. Wentworth, and D. P. Neikirk, "Twin slot antenna structures integrated with microbolometer detector for 94 GHz imaging," *Microwave and Optical Technology Letters*, Vol. 4, 15–19, 1999.
3. Rahman, A., E. Duerr, G. De Lange, and Q. Hu, "Micromachined room-temperature microbolometer for mm-wave detection and focal-plane imaging arrays," *SPIE Proceedings*, 122–133, April 1997.
4. Miller, A. J., A. Luukanen, and E. N. Grossman, "Micromachined antenna-coupled uncooled bolometers for terahertz imaging," *SPIE Proceedings*, 18–24, April 2004.
5. Milkov, M., "Millimeter-wave imaging system based on antenna-coupled bolometers," Master of Science Thesis, University of California Los Angeles, 2000.
6. Deal, W. R., L. Yujiri, M. Siddiqui, and R. Lai, "Advanced MMIC for passive millimeter and submillimeter wave imaging," *IEEE International Solid-state Circuits Conference*, 572–622, February 2007.
7. Kruse, P. W., *Uncooled Thermal Imaging*, SPIE Press, USA, 2001.
8. Dereniak, E. L. and G. D. Boreman, *Infrared Detectors and Systems*, Wiley Interscience, USA, 1996.
9. Kobayashi, H., M. Youki, and Y. Yasouka, "Effects of substrate thickness on the gain of millimeter and submillimeter wave slot antennas," *Electronics and Communications in Japan*, Vol. 80, 1–10, 1997.